ISSN 2229-5518

Robotic Configuration for Paralyzed Swing Leg with Effort Minimization of Stance Hip Torques and Bounded Stance Hip Orientation

A. Chennakesava Reddy, B. Kotiveerachari, P. Rami Reddy

Abstract— This research work was aimed at an alternate approach for walking and training the paralyzed leg with a robot attached to the pelvis. The dynamic properties considered in this work were mass, center of gravity, moments of inertia of each link and the friction at each joint. The least square method was employed to identify the dynamic properties after exciting the robot and collecting the data of joint positions, velocities, accelerations and applied forces. A robot attached to the pelvis was employed to control the stepping motion of a paralyzed person suspended on a treadmill. In this configuration the large swivel motion was eliminated. A reasonable swing motion was achieved by limiting excessive hip swivel. This robot configuration would need large amount of effort to shift the stance hip to complete a gait.

Index Terms— Robot, paralyzed leg, pelvis, trademill, walking motion.

1 INTRODUCTION

HUMAN walking is a smooth, highly coordinated, rhythmical movement by which the body moves step by step in the desired direction. Damage in walking ability is frequent after the heart attack and spinal cord injury. The clinical stepping motion training is too little because the training is labor concentrated. Many therapists are obligatory to control the pelvis and legs. Body weight supported (BWS) training has shown assurance in enhancing walking after spinal cord injury [1]. The technique involves suspending the patient above a treadmill to partly relieve the body weight, and physically supporting the legs and pelvis while moving in a walking pattern. Patients who be given this therapy can considerably increase their independent walking ability [2], [3]. This technique works by force, position, and touch sensors in the legs during stepping in a repetitive manner, and that the circuits in the nervous system learn from this sensor input to generate walking style. Kinematic approaches for simulating human walking have been illustrated by various researchers over the years [4], [5], [6].

A difficulty in automating BWS training is that the required amount of forces at the pelvis and legs are unknown. In the field of computer animation, because of the complex hierarchical structure of the human being, most of the research in motion control of human beings has been devoted to ways of reducing the amount of specification necessary to achieve a desired motion. Bruderlin and Calvert [7] have proposed procedural animation techniques to animate personalized human locomotion. In their system, three locomotion parameters, step length, step frequency and velocity, are used to specify the basic locomotion stride. Then, additional locomotion attributes are added at different levels of the motion control hierarchy to individualize the locomotion. Phillips and Badler [8] have implemented an inverse kinematics algorithm to generate motions. Minimization of energy described by the constraints is used to choose the set of joint angles among the multiple inverse kinematics solutions. Hodgins et al. [9] have introduced a dynamic approach to animate human running. The control algorithm is based on a cyclic state machine, which determines the proper control actions to calculate the forces, and torques that satisfy the requirements of the task and input from the user.

The BWS training with robotics is an attractive as it improves the training. This article aims at an alternate approach toward generating strategy for developing dynamic motion planning for walking and training the paralyzed leg with a robot attached to the pelvis. The robotic configuration is swing leg with effort minimization of all joints. This configuration is studied to determine a practical gait trajectory using the optimization technique. The robot configuration as shown in figure 1 is used to assist the paralyzed leg and to simulate the walking pattern of the normal leg.

2 REHABILITATION ROBOT CONFIGURATION

Basically, all normal people walk in the same way. From human gait observations [10], the differences in gait between one person and another occur mainly in movements in the coronal and transverse planes. While walking, the position and orientation of legs change as shown in figure 2. In

- *Professor, Department of Mechanical Engineering, JNTUH College of Engineering, Kukatpally, Hyderabad – 500 085, Telangana, India*
  acreddy@jntuh.ac.in, 09440568776
- *Professor, Department of Mechanical Engineering, National Institute of Technology, Warangal, Telangana, India*
- *Former Registrar, JNT University, Kukatpally, Hyderabad – 500 085, Telangana, India.*

consequence, the rehabilitation robot configuration is defined by the author in his research work [11]. The rehabilitation robot is described kinematically by giving the values of link length, link twist, joint distance and joint angle. The rehabilitation robot transformation matrices are very vital for the dynamic analysis.

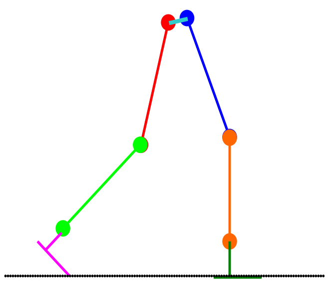

Fig. 1. Rehabilitation robot to represent normal legs.

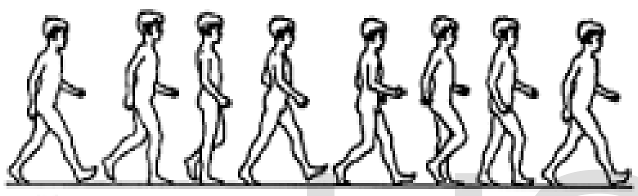

Fig. 2. Change of position and orientation of legs during walking.

3 METHODOLOGY

The position and orientation of frame i relative to that of frame (i–1) are given by

$$T_{0,n}(q_1,q_2,.....q_n) = T_{0,1}(q_1)T_{1,2}(q_2)\ .... \ T_{n-1,n}(q_n) \tag{1}$$

where q_i is the joint variable for link i.

The mapping between the joint velocities and the end-effector velocities is defined by the differential kinematics equation

$$V_e = \begin{bmatrix} \omega_e \\ v_e \end{bmatrix} = J_e(q)\dot{q} \tag{2}$$

where Ve is the spatial velocity of the end-effector; we and ve the angular and linear velocities of the end-effector, respectively; $\dot{q}$ the generalized velocity of the robot manipulator; and Je the Jacobian matrix. The Jacobian can be expressed entirely in terms of the joint screws mapped into the base frame. Each column of $J_e^s(q)$ depends only on q1, q2, . . . q_{i-1}. In other words, the contribution of the ith joint velocity to the end-effector velocity is independent of the configuration in the manipulator. The instantaneous spatial velocity of the end-effector is given by the twist

$$V_e^s = \left(\dot{T}_{0,n} T_{0,n}^{1}\right) = J_e^s(q)\dot{q} \tag{3}$$

where $J_e^s \in \Re^{6xn}$ is called the spatial Jacobian.

The spatial Jacobian can be expressed entirely in terms of the joint screws mapped into the base frame

$$J_e^s(q) = \left[Ad_{T0,1}S_1 Ad_{T0,2}S_2 ... Ad_{T0,n}S_n\right] \tag{4}$$

Each column of $J_e^s(q)$ depends only on q1, q2, . . . qi-1. In other words, the contribution of the ith joint velocity to the end-effector velocity is independent of the later configuration in the manipulator. The body Jacobian J_e^b is defined by the relationship

$$V_e^b = \left(T_{0,n}^{-1}\dot{T}_{0,n}\right)^v = \sum\left(T_{0,n}^{-1}\frac{\partial T_{o,n}}{\partial q_i}\right)^v \dot{q}_i = J_e^b(q)\dot{q} \tag{5}$$

The body Jacobian can be expressed as follows

$$J_e^b = \left[Ad_{T_{1,n}^{-1}}S_1 \quad Ad_{T_{2,n}^{e}}S_2 \ \ldots \ Ad_{T_{n-1,n}^{-1}}S_{n-1}S_n\right] \tag{6}$$

The body Jacobian can be expressed entirely in terms of the joint screws mapped into the end-effector frame. It maps the joint velocities into the corresponding spatial velocity of the end-effector in the end-effector frame. The spatial and body Jacobians are related by the adjoint transformation

$$J_e^s(q) = AD_{T_{0,n}} J_e^b \tag{7}$$

The dynamic equations of open-chained robot manipulators can be expressed in the general form

$$H(q)\ddot{q} + h(q,\dot{q}) = \tau \tag{8}$$

which relates the applied joint forces τ to the joint positions q and their time derivatives $\dot{q}$ and $\ddot{q}$. *H*(*q*) is the mass or inertia matrix and $h(q,\dot{q})$ contains the centrifugal, Coriolis, gravitational and frictional forces.

The Newton-Euler recursive algorithm of the inverse dynamics is as follows:

- Initialization

$$V_0, \dot{V}_0, F_{n+1} \tag{9}$$

- Forward recursion: *i* = 1 *to n*

$$V_i = Ad_{T_{i-1,i}^{-1}}V_{i-1} + S_i\dot{q}_i \tag{10}$$

$$\dot{V}_i = Ad_{T_{i-1,i}^{-1}}\dot{V}_{i-1} + S_i\ddot{q}_i + ad_{v_i}S_i\dot{q}_i \tag{11}$$

- Backward recursion: *i* = *n to* 1

$$F_i = Ad^*_{T_{i-1,i}^{-1}}F_{i+1} + J_i\dot{V}_i - ad^*_{v_i} + J_i\dot{V}_i - ad^*_{v_i}J_iV_i \tag{12}$$

$$\tau_i = S_i^T F_i + f_{ci}\,\mathrm{sgn}(\dot{q}_i) + f_{vi}\dot{q}_i \tag{13}$$

In this algorithm, the index i represents the ith link frame counted from the base frame (i = 0). The joint screw, spatial velocity, spatial acceleration and spatial force are written as S, V, $\dot{V}$ and $F \in se(3)$, respectively. Particularly, V_0 and $\dot{V}_0$ represent the spatial velocity and acceleration of the base, respectively, while Fn+1 represents the external spatial force on the last link or end-effector. $T_{i-1,i} \in SE(3)$ denotes the transformation from the (i – 1)th link frame to the ith link frame. The joint velocity, acceleration, force and the Coulomb and viscous frictions are written as $\dot{q}$, $\ddot{q}$, τ, f_c and $f_v \in \Re$, respectively. And J is the spatial inertia matrix

$$J_i = \begin{bmatrix} I_i - m_i\hat{r}_i^2 & m_i\hat{r}_i \\ -m_i\hat{r}_i & m_i \bullet 1 \end{bmatrix} \quad (14)$$

where mi and Ii are the mass and inertia of the i^{th} link, respectively; r_i is a vector from the origin of the ith link frame to the center of mass of ith link; $\hat{r}_i$ is the skew symmetric matrix formed by ri using the notation from the last chapter; and 1 is an identity matrix. The spatial velocity and force are

$$V_i = \begin{bmatrix} w_i \\ v_i \end{bmatrix} \text{ and } F_i = \begin{bmatrix} m_{ti} \\ f_{ti} \end{bmatrix} \quad (15)$$

where w, v, mt and ft are the angular velocity, linear velocity, moment and force, respectively. This recursive formulation shows how the spatial velocity and acceleration propagate forwards from the base to the end-effector and how the spatial force propagates backwards from the end-effector to the base.

Featherstone's [12] articulated-body method supplies an efficient solution to the forward dynamics problem. Featherstone has shown that the equations of motion of each link can be expressed as follows:

$$F_i = \hat{J}_i\dot{V}_i + \hat{F}_i \quad (16)$$

where $\hat{J}_i$ is the articulated-body inertia of link i, and $\hat{F}_i$ is the bias force associated with link i. It is assumed that a spatial force Fn-1 is applied to the articulated body. From the Newton-Euler recursive algorithm, it follows the equations of motion of each link

$$F_n = J_nV_n - ad^*_{V_n}J_nV_n \quad (17)$$

$$F_{n-1} = Ad^*_{T^{-1}_{n-1,n}}F_n + J_{n-1}\dot{V}_{n-1} - ad^*_{V_{n-1}}J_{n-1}V_{n-1} \quad (18)$$

The articulated-body method can be applied to solve not only the forward dynamics but also the inverse dynamics.

In the present work, the hybrid dynamics problem was defined as a system of equations for articulated bodies in which either the applied force or the joint acceleration for each joint was known.

The hybrid dynamics algorithm is as follows:

- Initialization

$$V_0, \dot{V}_0, F_{n+1}, F_{b_{n=+1}} = F_{n+1}, \hat{J}_{n+1} = 0, \hat{J}_{b_{n+1}} = 0, b_{n+1} = 0 \quad (19)$$

- Forward recursion: $i = 1 \ to \ n$

$$V_i = Ad_{T^{-1}_{i-1,i}}V_{i-1} + S_i\dot{q}_i \quad (20)$$

- Backward recursion $i = n \ to \ 1$

$$\hat{J}_i = J_i + Ad^*_{T^{-1}_{i,i+1}}J_{b_{i+1}}Ad_{T^{-1}_{i,1+1}} \quad (21)$$

$$\hat{F}_i = -ad^*_{V_i}J_iV_i + Ad^*_{T^{-1}_{i,i+1}}\left(F_{b_{i+1}} + \hat{J}_{i+1}S_{i+1}b_{i+1}\right) \quad (22)$$

$$F_{bi} = \hat{F}_i + \hat{J}_i ad_{V_i}S_i\dot{q}_i \quad (23)$$

$$J_{bi} = \begin{cases} \hat{J}_i & i \in I^a \\ \hat{J}_i - \hat{J}_iS_iS_i^T\hat{J}_i \big/ S_i^T\hat{J}_iS_i & i \in I^p \end{cases} \quad (24)$$

$$b_i = \begin{cases} \ddot{q}_i & i \in I^a \\ \left(\tau_i - S_i^TF_{bi}\right) \big/ S_i^T\hat{J}_iS_i & i \in I^p \end{cases} \quad (25)$$

- Forward recursion: $i = 1 \ to \ n$

$$\begin{cases} \tau_i = S_i^T\left(F_{bi} + \hat{J}_iAd_{T^{-1}_{i-1,i}}\dot{V}_{i-1} + \hat{J}_iS_ib_i\right) & i \in I^a \\ \ddot{q}_i = b_i - \left(S_i^T\hat{J}_iAd_{T^{-1}_{i-1,i}}\dot{V}_{i-1}\right) \big/ \left(S_i^T\hat{J}_iS\right)_i & i \in I^p \end{cases} \quad (26)$$

$$\dot{V}_i = Ad_{T^{-1}_{i-1,i}}\dot{V}_{i-1} + S_i\ddot{q}_i + ad_{V_i}S_i\dot{q}_i \quad (27)$$

The B-spline curve is used to the joint trajectories [13]. The B-spline curve, $q \in \Re$ is written as

$$q(t,p) = \sum_{j=0}^{m} p_jB_{j,k}(t) \quad (28)$$

where $p = \{p_0, \ldots p_m\}$, with , are the control points and $B_{j,k}$ is the B-spline basis function. The index k defines the order of the basis polynomial, e.g. k = 4 for a cubic one or k = 6 for a quintic one. The semi-infinite constraints are transformed into a set of linear inequalities by exploiting the convex hull property.

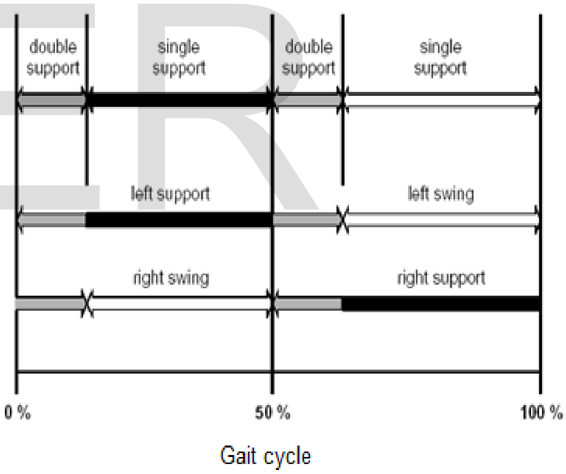

Fig. 3. Gait cycle of human walking.

1 HUMAN MODEL AND WALKING MOTION

For studying the motion of the legs, the head, torso, pelvis, and arms were combined into a single rigid body (upper trunk). The walking gait cycle (figure 3) was assumed to be bilaterally symmetric [14]. The left-side stance and swing phases were assumed to be identical to the right-side stance and swing phases, respectively. Thus, only one-half of the gait cycle was simulated in this study. The stance hip was modeled as a two degrees-of-freedom (DOF) universal joint rotating about the x- and y-directions. The upper trunk was fixed about the z-axis. The swing hip was modeled as a 3 DOF ball joint rotating about axes in the x-, y-, and z- directions. The

IJSER

ISSN 2229-5518

knee and ankle were modeled as 1 DOF hinge joints about the z-axis.

TABLE 1
Link Lengths

l_{hip}	$l_{upper\ leg}$	$l_{lower\ leg}$	l_{foot}	l_{toe}	l_{heel}
0.15 m	0.47 m	0.49 m	0.08	0.18 m	0.07 m

TABLE 2
Dynamic Properties of Human Model

Link	Mass, Kg	Inertia, Kg-m2	Center of Mass, m
Upper Trunk	46.05	$\begin{bmatrix} 3.23 & 0 & 0 \\ 0 & 0.78 & 0 \\ 0 & 0 & 2.76 \end{bmatrix}$	$\begin{Bmatrix} -0.001 \\ 0.360 \\ 0 \end{Bmatrix}$
Upper Leg	9.54	$\begin{bmatrix} 30.16 & 0 & 0 \\ 0 & 0.035 & 0 \\ 0 & 0 & 1.15 \end{bmatrix}$	$\begin{Bmatrix} -0.025 \\ -0.170 \\ 0.007 \end{Bmatrix}$
Lower Leg	3.56	$\begin{bmatrix} 0.064 & 0 & 0 \\ 0 & 0.006 & 0 \\ 0 & 0 & 0.062 \end{bmatrix}$	$\begin{Bmatrix} -0.005 \\ -0.207 \\ 0.019 \end{Bmatrix}$
Foot	1.44	$\begin{bmatrix} 0.003 & 0 & 0 \\ 0 & 0.009 & 0 \\ 0 & 0 & 0.007 \end{bmatrix}$	$\begin{Bmatrix} 0.044 \\ -0.040 \\ 0.010 \end{Bmatrix}$

IJSER

Motion capture data of major body segments for an unimpaired person during treadmill walking was obtained using a video-based system at FESTO Pvt.Ltd, Bangalore. The frequency of motion capture was 50 Hz. External markers were attached to the body at the antero-superior iliac spines (ASISs), knees, ankles, tops of the toes, and backs of the heels [15]. The link lengths and joint orientations are shown in Table 1. The human subject was 1.95 m tall and weighed 70 kg. Passive torque-angle properties of the hip, knee, and ankle joints were measured for the subject with a Biodex active dynamometer. Joints were measured in a gravity-eliminated configuration. The dynamic properties of the human model are given in Table 2.

The joints were modeled as nonlinear springs in which the joint torque was a polynomial function of the joint angle. A least squares method was used to best-fit polynomials. Third order polynomial function was used for the torque-angle property of each joint. A polynomial of order 7 was used to the ankle joint data. The polynomial equations for curves are mentioned as follows:

Hip external/internal rotation $\left(\quad 60^0, 60^0 \right)$

$$\tau_m = \quad 0.6837 \quad 0.7621q + 0.9772q^2 \quad 2.2620q^3 \tag{29}$$

Hip abduction/adduction $\left(\quad 50^0, 30^0 \right)$

$$\tau_m = \quad 0.0542 \quad 0.8266q \quad 6.0205q^2 \quad 29.0271q^3 \tag{30}$$

Hip extension/flexion $\left(\quad 35^0, 70^0 \right)$

$$\tau_m = 1.0863 + 1.5721q + 6.3488q^2 \quad 23.0405q^3 \tag{31}$$

Knee flexion/extension $\left(\quad 140^0, 0^0 \right)$

$$\tau_m = \quad 24.9343 \quad 53.1584q \quad 37.5211q^2 \quad 9.8685q^3 \tag{32}$$

Ankle plantar/dorsal flexion $\left(-52^0, 46^0 \right)$

$$\begin{aligned} \tau_m = {} & 0.1305 + \quad 3.99564q + 1.5596q^2 \quad +4.7881q^3 + 2.4229q^4 \\ & + 6.2372q^5 + \quad 5.6802q^6 + \quad 19.5304q^7 \end{aligned} \tag{33}$$

In addition to the polynomial function, a nonlinear spring-damper system was used to place a hard limit on joint movement when it is close to its upper and lower bounds.

$$\tau_{sd} = \begin{cases} -\beta\left(10^4 (q - q_2) + 5x10^2 \dot{q}\right) & if \quad q \geq q_2 \\ -\beta\left(10^4 (q - q_1) + 5x10^2 \dot{q}\right) & if \quad q \leq q_1 \\ 0 & \text{otherwise} \end{cases} \tag{34}$$

where

$$\beta = \begin{cases} 6x10^5 (q - q_2)^5 - 1.5x10^5 (q - q_2)^4 + 10^4 (q - q_2)^3 & if \quad q_2 + 0.1 \geq q \geq q_2 \\ -6x10^5 (q - q_1)^5 - 1.5x10^5 (q - q_1)^4 + 10^4 (q - q_1)^3 & if \quad q_1 - 0.1 \geq q \geq q_1 \\ 1 & otherwise \end{cases}$$

The function τ_{sd} is c^2 continuous in order to be used in the computation of the analytical gradient in the dynamic motion optimization. Four steps at three different treadmill walking speeds (1.75, 1.25 and 0.75 m/sec) were obtained from motion capture. The swing motion was considered to be an optimal control problem as follows:

$$\min_{\tau(t)} J_c = \frac{1}{2} \int_0^{t_f} \sum_{i=4}^{10} w_{ei} \tau_i^2 \, dt \tag{35}$$

$$\text{s.t} \qquad H(q)\ddot{q} + h(q, \dot{q}) = \tau + \tau_{msd} \tag{36}$$

$$q(0) - q_0, \quad \dot{q}(0) = \dot{q}_0 \tag{37}$$

$$q(t_f) - q_f, \quad \dot{q}(t_f) = \dot{q}_f \tag{38}$$

where τ_1, τ_2 and τ_3 are the generalized forces associated with the translation of the stance hip (and are not included in the cost function since the position of the stance hip was specified by the motion capture data); τ_4 and τ_5 are the moments corresponding to the two rotations of the stance hip (controlled by the robot); τ_6, τ_7 and τ_8 are the swing hip moments (corresponding to hip abduction/adduction and extension/flexion, external/internal rotation, respectively); τ_9 and τ_{10} correspond to knee and ankle rotation moments, respectively; and w_{ei}'s are positive weighting coefficients. $\tau_6 \sim \tau_{10}$ were assumed zero for the impaired leg. $\tau_{msd4} \sim \tau_{msd10}$ were modeled as nonlinear spring-damper muscle systems while $\tau_{msd1} \sim \tau_{msd3}$ were zero since no muscular force is needed for the linear translation of the stance hip.

ISSN 2229-5518

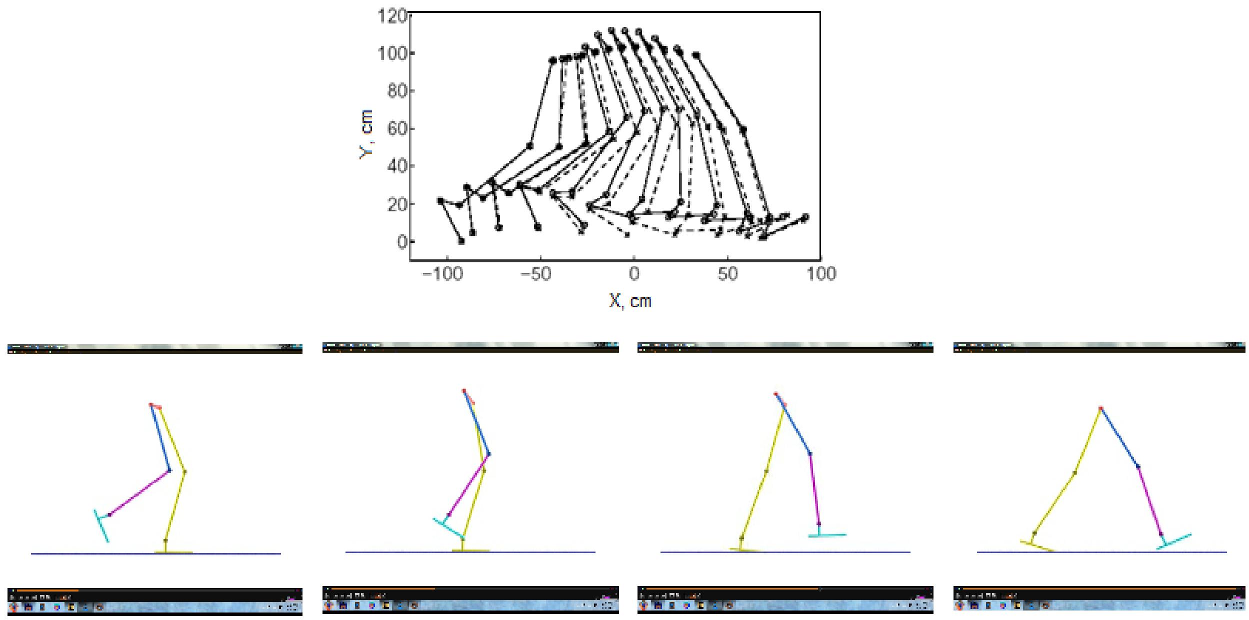

Fig. 4. Gait for duration of 0.45 sec.

s

2 RESULTS AND DISCUSSION

The joint positions are shown in figure 4 & 5. Solid lines represent the simulated data. The dashed lines signify experimental data. In this configuration the large swivel motion was eliminated. The stance hip external/internal rotation was restricted within ±300 range. A reasonable swing motion was achieved by limiting excessive hip swivel. There was no collision between the leg and the ground at about x = 0 (mid-stride) if the ground was not neglected.

IJSER

ISSN 2229-5518

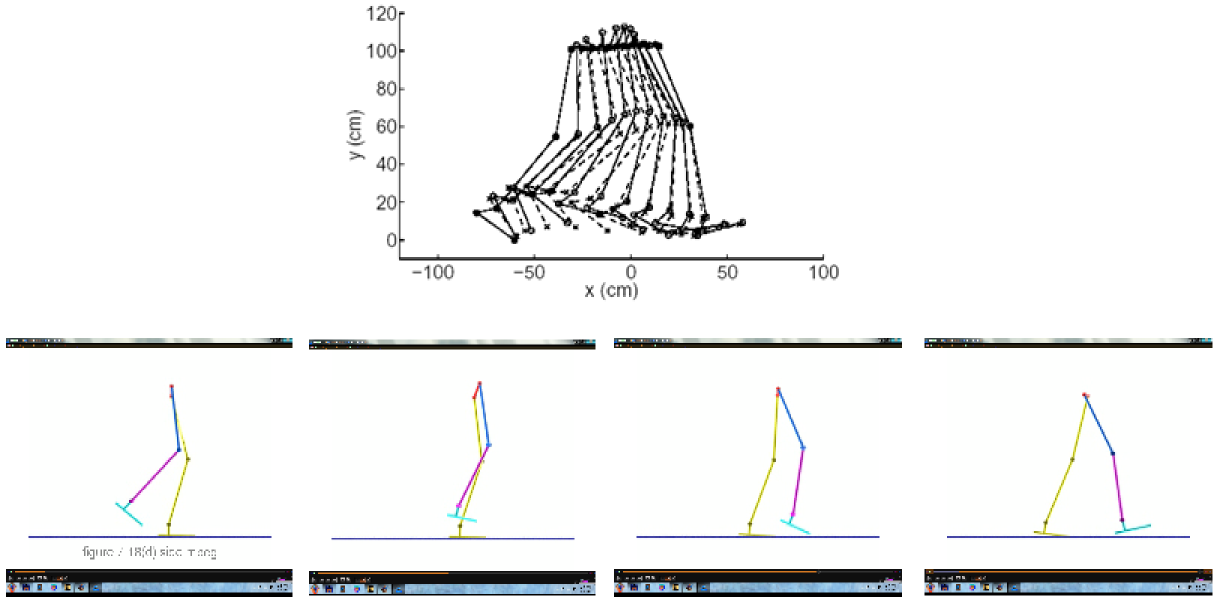

Fig. 5. Gait for duration of 0.60 sec

IJSER

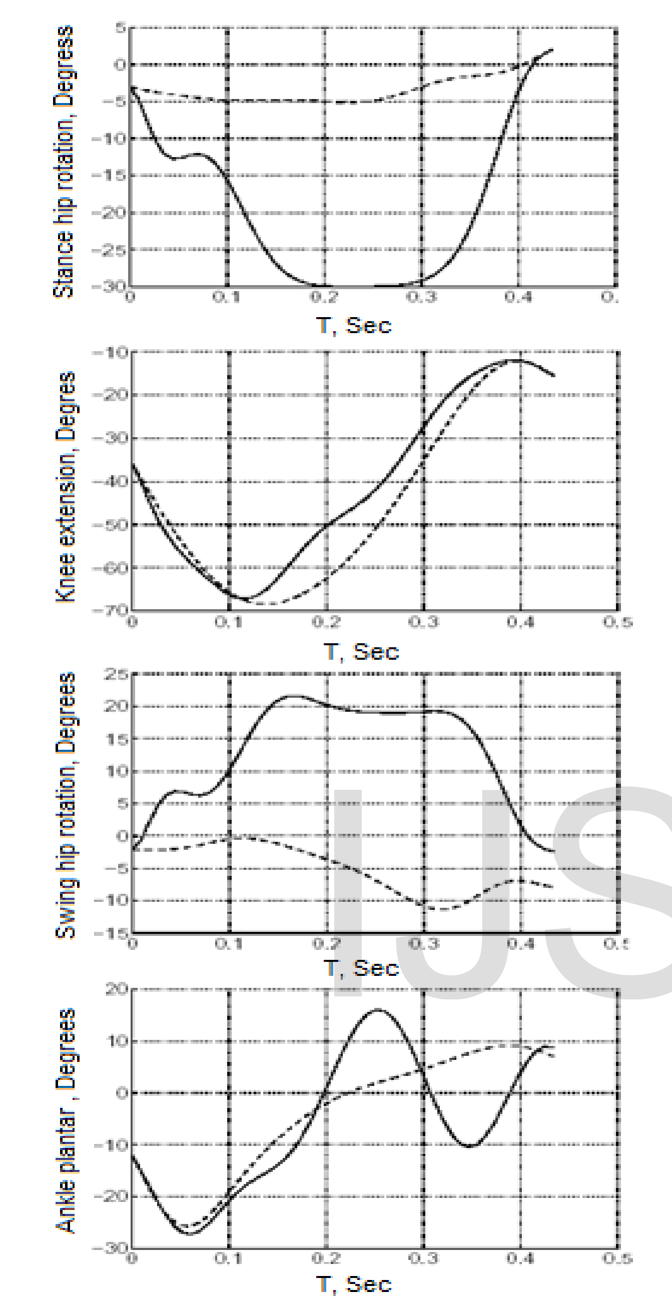

Fig. 6. The joint motions (duration 0.45 sec).

The joint motions of the gait for duration 0.45 sec are shown in figure 6. The solid lines show the joint motions from the algorithm used and the dashed lines are the joint motions recorded from the motion capture system. The swing hip rotation was found to be greater from the results obtained from the algorithm than those taken from the motion capture for gait duration of 0.45 sec. Also, the stance hip rotation was found to be lesser from the results obtained from the algorithm than those taken from the motion capture for gait duration of 0.45 sec. the swing hip and stance hip rotations obtained from the algorithm were nearly same to those taken from the motion capture for gait duration of 0.60 sec. The bound limits to the swivel of the pelvis which causes the underactuated model in this configuration has yield a larger final position error.

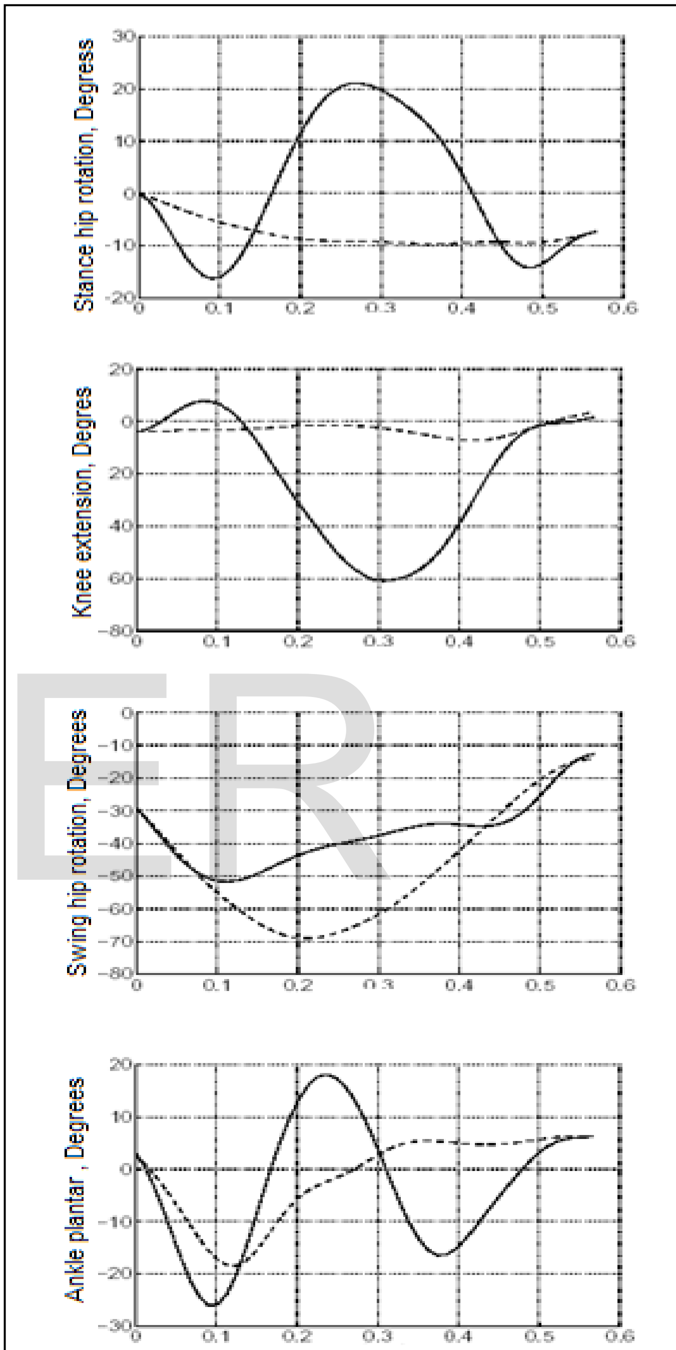

Fig. 7. The joint motions (duration 0.45 sec).

Figures 8 & 9 demonstrate that most of the effort went into tilting the pelvis, i.e. abducting the stance hip, due to working against gravity. It also shows that this robot configuration would need large amount of effort to shift the stance hip to complete a gait.

IJSER

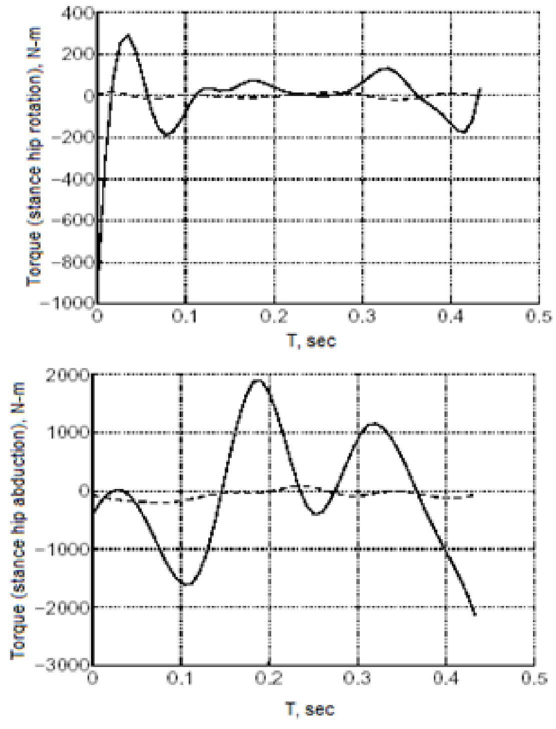

Fig. 8. Joint torques (for duration of 0.45 sec).

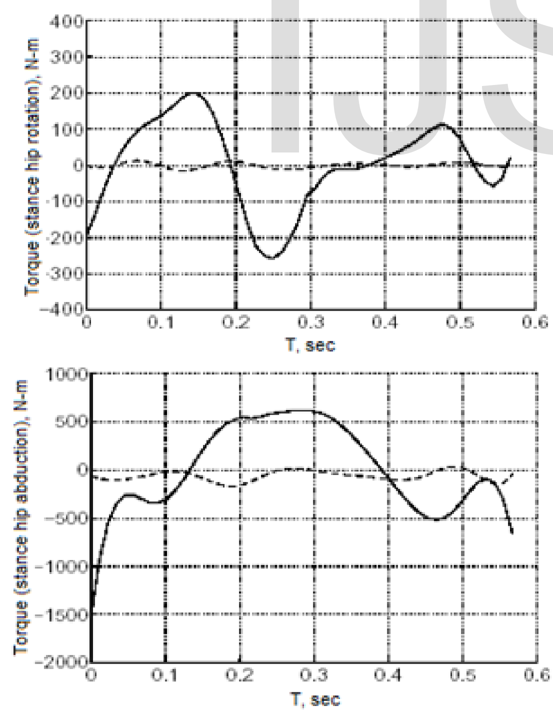

Fig. 8. Joint torques (for duration of 0.60 sec).

3 CONCLUSIONS

Walking motion was generated for a robot attached to the pelvis of a paralyzed person suspended on a treadmill. A leg swing motion was created by moving the pelvis. In this robot configuration the large swivel motion was eliminated. There was no collision between the leg and the ground at about x = 0 (mid-stride) if the ground was not neglected. Most of the effort went into tilting the pelvis, i.e. abducting the stance hip, due to working against gravity.

REFERENCES

[1] I. Wickelgren, “Teaching the spinal cord to walk,” Science, vol.279, pp.319–321, 1998.

[2] H. Barbeau, K. Norman, J. Fung, M. Visintin, and M. Ladoucer, “Does neuro-rehabilitation play a role in the recovery of walking in neurological populations,” Annals New York Academy of Sciences, vol.860, pp.377–392, 1998.

[3] H. Ko, and N.I. Badler, “Straight-line walking animation based on kinematic generalization that preserves the original characteristics,” Graphics Interface, vol.28, pp.9-16, 1993.

[4] N. Boulic, M. Thalmann and D. Thalmann, “A Global Human Walking Model with Real- time Kinematic Personification,” Visual Computer, vol.6, pp.344-358, 1990.

[5] T.W. Calvert, and J. Chapman, “Aspects of the kinematic simulation of human movement:, IEEE Computer Graphics and Applications, vol. 2, pp.41-50, 1982.

[6] A.C. Reddy, B. Kotiveerachari, P.R.Reddy, “Dynamic trajectory planning of robot arms”, Journal of Manufacturing Technology, vol.3, no.3, pp.15-18, 2004.

[7] A. Bruderlin, and T.W. Calvert, “Interactive Animation of Personalized Human Locomotion,” GI’93, vol.28, pp.17-23, 1993.

[8] C. B. Phillips, N.I. Badler, and B.L.Webber, “Simulating humans,” Oxford University Press, 1993.

[9] J. K. Hodgins, W.L. Wooten, A. C. Brogan and J.F. O’Brien, “Animating Human Athletics,” Computer Graphics, vol.29, pp.71-78, 1995.

[10] M. P. Murray, A. B. Drought, and R. C. Kory, “Walking patterns of normal men,” Journal of Bone and Joint Surgery, vol.46A, pp. 335-359, 1964.

[11] A.C. Reddy, “Studies on synthesis and optimization of robotic configurations used for training of paralyzed person through dynamic parameter consideration,” Ph.D Thesis, 2007.

[12] R. Featherstone, “Robot Dynamics Algorithms” Kluwer Academic Publishers, Norwell, MA, 1988.

[13] Chennakesava R Alavala, “CAD/CAM: Concepts and Applications,” PHI Learning Private Limited, New Delhi, 2008.

[14] A. Chennakesava Reddy and B. Kotiveerachari, “Different methods of robotic motion planning for assigning and training paralysed person,” Journal of Institution of Engineers, vol. 88, pp.37-41, 2008.

[15] A. Chennakesava Reddy, G.S. Babu, “Dynamic mechanisms of kneecap, compliant ankle and passive swing leg to simulate human walking robot,” International Journal of Advanced Mechatronics and Robotics, vol.3, pp.1-7, 2011.

IJSER